

# Thin Films and Coatings

## MS.5.117

### Competing Magnéli-like phases driven by substrate-induced strain in TiO<sub>2</sub> anatase thin films

R. Ciancio<sup>1</sup>, A. Vittadini<sup>2,3</sup>, A. Selloni<sup>4</sup>, C. Aruta<sup>5</sup>, F. Miletto Granozio<sup>6,7</sup>, U. Scotti di Uccio<sup>6,7</sup>, G. Rossi<sup>1,8</sup>, E. Carlino<sup>1</sup>

<sup>1</sup>CNR-IOM, Trieste, Italy

<sup>2</sup>CNR-ISTM, Padova, Italy

<sup>3</sup>CR-INSTM, Padova, Italy

<sup>4</sup>Princeton University, CNR, Princeton, United States

<sup>5</sup>CNR-SPIN, Rome, Italy

<sup>6</sup>CNR-SPIN, Naples, Italy

<sup>7</sup>University of Naples "Federico II", Naples, Italy

<sup>8</sup>University of Milan, Milan, Italy

ciancio@iom.cnr.it

Keywords: anatase, HRTEM and STEM/HAADF, Density Functional Theory calculations

We used high-resolution transmission electron microscopy (HRTEM) experiments and simulation together with density functional theory (DFT) calculations to characterize the structure and defects in LaAlO<sub>3</sub>-supported TiO<sub>2</sub> anatase thin films. Bright field TEM shows that the film is 40 nm thick and is split into two adjacent slabs of about 20 nm thickness each, characterized by different diffraction contrast (see Figure 1a). Closer HRTEM inspection shows that the two slabs have a modulated structure typical of the existence of crystallographic shear (CS) planes. In particular, we detected (103)- and (101)-oriented shear plane structures in the outer film region and in proximity of the film/substrate interface, respectively (see Figure 1b). Diffractograms taken over the two CS regions and displayed in Figure 1c and 1d, respectively, show a typical multiple-peak pattern, which indicates a superstructure-like behavior originating from the CS planes and defining two new superlattices. STEM/HAADF and Energy Dispersive X-ray Spectroscopy (EDXS) revealed the presence of Al interdiffusion from the substrate into the first 20 nm of the film[1].

By combining HRTEM results and relevant image simulations with DFT calculations we determined the atomic structure of the CS planes and show that they are based on the cubic TiO structure resembling the classical rutile-derived Ti<sub>n</sub>O<sub>2n-1</sub> Magnéli phases[2]. Figure 2a shows a HRTEM image focused at the (103) CS region; in Figure 2b a simulated image obtained from the (103) CS optimized structural model at 6 nm thickness and 74-nm underfocus values is displayed. A very good agreement is found between experiment and simulation, as highlighted by line profiles across the intensity maxima along the relevant segments of the two images. Differently from the previous case, although the orientation and spacing of the (101) CS planes in the theoretical model agree with the experimental ones, a discrepancy is observed in the linear arrangement of the brighter contrast spots running along the [100] anatase direction, as shown by the line scan profiles taken across the intensity maxima of representative segments of the two images (Figure 3a and 3b). Such a discrepancy may be related to the Al interdiffusion measured by HAADF and EDXS from the substrate over the first 20 nm film region[1,2]. DFT-derived thermodynamic predictions provided information on the stability of the observed structures as well as on the relations to the growth dynamics and to the matching with the bare substrate. Interestingly, we found that the crossover in the film between the two region hosting the two different Magnéli-like phases corresponds to the transition from a three-dimensional (3D) to a two-dimensional (2D) growth mode in the film structure as observed by in-situ reflection high energy electron diffraction (RHEED) during film growth[3].

Based on the experimental and theoretical evidences, we proposed a model for the peculiar growth mode of the overlayer and drew conclusions on the role of cation interdiffusion on film nucleation providing an explanation for the relative predominance of (103) and (101) CS planes in the body of the film and close to the interface with the substrate, respectively.

Our results shed light on fundamental processes useful also for tailoring the heteroepitaxial growth of TiO<sub>2</sub> anatase for device applications. In particular, we unveiled new effects which might be tailored to engineer new heterostructures with ad-hoc functionalities related to fundamental growth mechanisms.

1. R. Ciancio, E. Carlino, C. Aruta, D. Maccariello, F. Mileto Granozio and U. Scotti di Uccio, *Nanoscale* 4 (2012) 91.
2. R. Ciancio, E. Carlino, G. Rossi, C. Aruta, U. Scotti di Uccio, A. Vittadini and A. Selloni, *Physical Review B* 86 (2012) 104110.
3. R. Ciancio, A. Vittadini, A. Selloni, R. Arpaia, C. Aruta, F. Mileto Granozio, U. Scotti di Uccio, G. Rossi and E. Carlino, submitted to *Journal of Nanoparticle Research*.

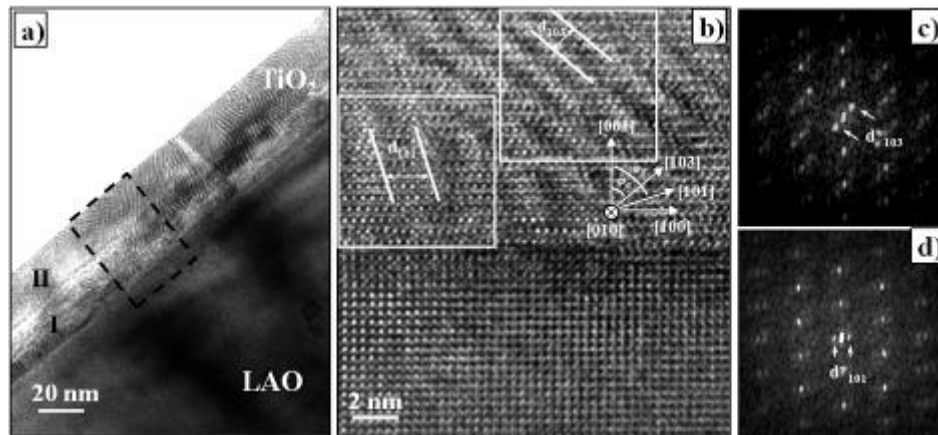


**Figure 1.** (a) Bright field TEM image of the TiO<sub>2</sub>/LAO film in the [010] TiO<sub>2</sub> zone axis showing the splitting of the film into adjacent regions (I and II) with different diffraction contrast. (b) HRTEM image of the TiO<sub>2</sub>/LAO interfacial region, taken in the [010] zone axis, of the film showing the presence of two types of modulations characterized by different spacing ( $d_{101}$  and  $d_{103}$ ). Diffractograms taken over the region containing (c) (103) and (d) (101) CS planes. The satellite peaks around the (000) reflection are indicated by arrows in the two diffractograms.

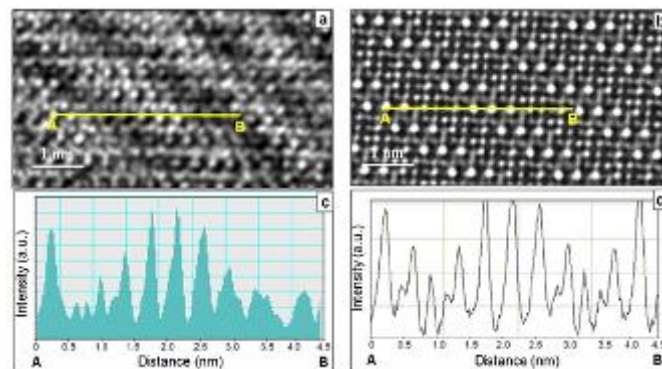


**Figure 2.** (a) HRTEM image focused at the film region containing (103) shear planes and taken in the [010] zone axis of the anatase film. (b) Simulated image obtained from the (103) CS modeled structure at 6 nm thickness and 74-nm underfocus values. Line scans across image intensity maxima calculated along the line of the (c) experimental and (d) simulated image.

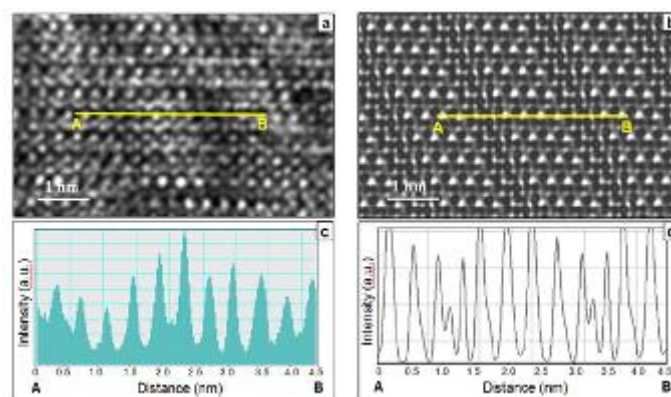


**Figure 3.** (a) HRTEM image focused at the film region containing (101) shear planes and taken in the [010] zone axis of the anatase film. (b) Image simulation calculated from the (101) CS modeled structure obtained at 6 nm thickness and 74-nm underfocus values. Line scans across phase maxima calculated along the line of the (c) experimental and (d) simulated image.